Hybrid TiO_2-$SiMgO_X$ Composite for Combined Chemisorption and Photocatalytic Elimination of Gaseous H_2S

Søren Birk Rasmussen[a], Raquel Portela[b], Silvia Suárez[b], Juan Manuel Coronado[b#], María-Luisa Rojas-Cervantes[c], Pedro Avila[a], Benigno Sánchez[b]*

[a] Instituto de Catálisis y Petroleoquímica. Calle Marie Curie, 2, 28049, Cantoblanco, Madrid, Spain.

[b] CIEMAT-PSA-Aplicaciones Ambientales de la Radiación Solar. Avda. Complutense, 22, Building 42, 28040, Madrid, Spain.

Present address: IMDEA Energía. 28933, Móstoles, Madrid, Spain.

[c] Dpto. Química Inorgánica y Química Técnica, UNED. Paseo Senda del Rey, 9, 28040, Madrid, Spain.

* benigno.sanchez@ciemat.es

ABSTRACT. Cheap natural sepiolite clay and TiO_2 in the anatase form can easily be converted into an efficient hybrid adsorbent/photocatalytic material, usable for H_2S and SO_2 capture and odor elimination. This can be achieved by extrusion of powder mixtures combined with coating of photocatalytically active titania. By means of the sorption capacity of the sepiolite it is possible to fixate gaseous sulfur species and by subsequent or simultaneous use of sunlight or artificial light sources, photocatalytic oxidation into oxidized sulfur compounds can be achieved without SO_2 release. The formation of such compounds as final products makes it possible to regenerate the composite material after saturation by washing with normal water. This technology constitutes an economically promising, sustainable, non-toxic, future method for H_2S elimination from the gas phase in sewage and wastewater treatment plants.

Keywords: H_2S, SO_2, oxidation, adsorption, TiO_2, sepiolite, photocatalysis.

INTRODUCTION

Increased urbanization and industrialization is followed by inherent drawbacks in terms of contamination and accumulation of waste material. Especially toxic compounds are becoming an environmental concern, which needs to be addressed by developing new sustainable technologies. In recent years, environmental legislation has imposed stringent limits on atmospheric emission levels. In particular, the release of foul smelling, toxic or corrosive compounds from water treatment plants have received much attention. The most important are reduced sulfur and nitrogen compounds, organic acids, aldehydes and ketones[1], with sulfur compounds being among the most polluting. For example, H_2S is toxic, corrosive[2], and generally considered an environmentally hazardous compound. Mercaptans, aromatic thiols, organic sulfides, etc. all contribute to odor related contamination as well.

The formation of H_2S from water treatment plants is associated with anaerobic conditions in collectors with low water flow and or high ambient temperatures. In these conditions sulfates present in the sewage water are reduced to sulfides by bacteria such as "Desulphovibrio Desulphuricans". This bacterium facilitates the oxidation of long chain organic acids present in the sewage water to acetic acid. The reaction is of the following type:

$$2CH_3\text{-}CHOH\text{-}COOH + SO_4^{2-} \rightarrow 2CH_3\text{-}COOH + H_2S + 2CO_2 + 2OH^- \quad [1]$$

Sulfides desorb from wastewater to the air as H_2S. To avoid H_2S desorption from water, the pH can be modified but the implementation of continuous cleaning systems for gas vapors, usually based on adsorption units, is preferred. These H_2S removal units require certain specific properties for the adsorbent material. Activated carbons are currently the adsorbents used in water treatment plants. They are often impregnated with caustic materials such as NaOH, KOH or otherwise modified.[3, 4] The foul smelling air from the sewage chambers are initially washed in scrubbers, during which they gain high levels of humidity, and are then blown

through the adsorbent bed.[5] H_2S thus reacts with the basic adsorbent and is immobilized by various oxidation reactions, which are accelerated by the presence of humidity.[6,7] A drawback of these caustic impregnated carbon systems is that hydrogen sulfide is oxidized to elemental sulfur,[7,8] which cannot very easily be regenerated.[9,10] Depending on the type of adsorbent and the surface sites, H_2S undergoes a number of transformations during its deposition on the solid surface:[11]

$$H_2S_{gas} \rightarrow H_2S_{ads} \quad [2]$$

$$H_2S_{ads} \rightarrow H_2S_{ads\text{-}liq} \quad [3]$$

$$H_2S_{ads\text{-}liq} \rightarrow HS^-_{ads} + H^+ \quad [4]$$

$$HS^-_{ads} + O^*_{ads} \rightarrow S_{ads} + OH^- \quad [5]$$

$$HS^-_{ads} + 3O^*_{ads} \rightarrow SO_{2\ ads} + OH^- \quad [6]$$

For the conversion of reduced species like sulfides into the more benign and regenerable compounds like SO_3^{2-} or SO_4^{2-} catalytically active surfaces are required. In this relation, photocatalytically active adsorbents are very interesting materials, since photocatalysis is considered an attractive and sustainable technology for elimination of pollutants either in aqueous media or in gas phase.[12] The photocatalytic process is especially adept for treatment of minor concentrations of contaminants in moderate/low effluent flows. TiO_2 is the classic photocatalytic material since it exhibits high photocatalytic activity.[13]

The mechanism for the photocatalytic degradation of H_2S is not fully understood. Two of the proposed reactions pathways described in the literature involve OH radicals[14] (eq 7) or molecular oxygen[15] (eq 8) to produce sulfates species:

$$H_2S + 8OH^{\bullet} \rightarrow SO_4^{2-} + 2H^+ + 4H_2O \quad [7]$$

$$H_2S + \frac{5}{2}O_2 + 2e \rightarrow SO_4^{2-} + 4H_2O \quad [8]$$

Further research in this field demonstrated the formation of SO_2 as reaction product.[16,17] The formation of SO_2

could be explained considering the following reaction.[18]

$$H_2S + 3OH^{\bullet} + O_2 \rightarrow SO_2 + \frac{3}{2}H_2O \qquad [9]$$

SO_2 is another toxic pollutant, and its release into the atmosphere should be avoided. The ideal photocatalytic process would be the transformation of H_2S into weakly adsorbed soluble sulfur species that facilitate the recovery of the photocatalytic activity by a simple rinsing step.

For industrial purposes immediate use of TiO_2 particles is not possible, unless the photocatalytic material is build into a conformed or supported material. There has been much interest in finding new methods for the deposition of TiO_2 as thin films.[19] Borosilicate glass conformed in various shapes has been extensively used for TiO_2 deposition. Although the most suitable conformation for treating large gas volumes are open channel monoliths, honeycomb structures present the drawbacks of channel-wall opacity and poor illumination efficiency have to be overcome.[20]

Untreated sepiolite, a fibrous magnesium silicate ($SiMgO_x$), is a light and inexpensive material frequently used as an adsorbent because of its high surface area and porosity.[21] This clay is extensively used as cat litters, for removal of pesticides, moisture control, and animal feedstuffs (additive E-562). According to Bellman et al. the sepiolite from Tolsa S.A (Madrid, Spain) exhibits low biological activity because of the short length of its fibers.[22] Moreover it is used as catalytic support since it improves the mechanical strengths of TiO_2- and Al_2O_3-based catalysts.[23] The exact catalytic role of sepiolite in such catalytic processes is not totally clear. In fact, it has been suggested that this silicate may play a role in the migration of oxygen species and hydrogen spillover.[24,] For photocatalytic processes, the diffusion of OH radicals on illuminated TiO_2 has been reported in different studies. Lee and Choi[25] found that generated OH radicals on the TiO_2 surface migrated beyond 80 µm to mediate the oxidation of carbon soot. Therefore it is likely that sepiolite might exhibit similar interesting properties.

In this work, ceramic plates based on $SiMgO_x$, or $SiMgO_X$ mixed with TiO_2 powder, were developed and

tested in the photocatalytic oxidation of H_2S. In a similar approach, conformed $SiMgO_X$ can be coated with TiO_2. These " conformed hybrid photocatalytic materials" represent an attractive method for abatement of pollutants.[26,27] The resulting removal will be bifunctional, based on chemisorption of pollutants on the adsorbent material followed by their diffusion towards the active photocatalytic centers. Earlier,[28,29] this concept has been proved for photocatalytic oxidation of TCE.

The implementation of this system for H_2S elimination should facilitate further oxidation (e.g. as in equation 6) of the toxic gaseous sulfur species into sulfites and sulfates. Therefore, the materials become easy to regenerate, since washing with pure water is sufficient. This will prevent the use of hazardous chemicals such as strong bases on-site at the water cleaning plants, and furthermore reduce maintenance costs and labor risks.

EXPERIMENTAL

Synthesis. Plated supports were made by extrusion of doughs prepared by kneading a mixture of TiO_2–anatase (G-5, Millenium) and $SiMgO_X$ (sepiolite, Tolsa S.A.) or pure $SiMgO_X$ with water. The optimum $TiO_2/SiMgO_X$ ratio selected to carry out this study was 1:1, since this combines good textural and mechanical properties.[30] The plate shaped materials were dried at room temperature for 48 h, then at 150°C for 12 h and finally treated at 500°C for 4h to obtain the desired crystalline phases. The resulting plates had the following dimensions: wall thickness 2 mm, geometric surface 19.76 cm^2 (2.6 x 7.6 cm).

Powder X-ray diffraction. Crystalline phases were determined by X-ray diffraction (XRD) on powdered samples with a PANalytical X´Pert Pro diffractometer with a nickel filter using a Cu $K_{\alpha 1}$ radiation with a wavelength of λ = 1.5406 nm. The spectra were measured over the 2Θ = 4-90° range with a 0.02° step with an acquisition rate of 2 s per step. Identification of the crystalline species was made out using the X' Pert Highscore Plus software.

N_2-Adsorption isotherms. Textural properties of the samples, i.e. specific surface area micro- and meso-pore volumes were analyzed by adsorption/desorption of nitrogen at –196°C, in a Sorptomatic apparatus from Thermo Electron Instruments. The samples were outgassed overnight at 300°C to a vacuum of less than 10^{-4} Torr to ensure that the surface was free from any loosely adsorbed species. All subsequent calculations were made subject to the outgassed weight of the sample. The BET method was used to determine the specific surface areas (S_{BET}) from the adsorption data in the linear portion of the isotherm located in the relative pressure range of 0.05– 0.30 p/p_0, typical for these samples.[31]

Mercury intrusion porosimetry (MIP). A CE Instruments Pascal 140/240 apparatus was used to determine pore volume over the range of 7.5 nm to 300 µm. The Washburn Equation[32] was used to analyze the pressure/volume data assuming a cylindrical non-intersecting pore model, taking the mercury contact angle and surface tension as 141° and 484 $m{\cdot}N{\cdot}m^{-1}$, respectively.[33] Samples were dried overnight at 150°C previous to the measurement to ensure that they were free from any loosely bound adsorbed species.

H_2S and SO_2 adsorption/chemisorption measurements. For tests of adsorptive capacities, the plated materials were gently crushed, sieved and the fraction of plates with sizes between 2-4 mm were transferred into a cylindrical reactor with Ø=10.7 mm and a bed height of 16 cm. Using a conventional flow rig, the dynamic adsorption capacities were determined in dry conditions using a concentration of approximately 100 ppm H_2S and flow rate, F = 1000 $ml{\cdot}min^{-1}$. The H_2S level in the outlet stream was continuously determined by a Varian CP4900 µ-GC. Immediately before and after each adsorption test, the inlet concentration was determined by letting the gas bypass the reactor for several minutes until a steady value was observed. A similar flow rig was used for SO_2 adsorption tests. Here a concentration of 730 ppm SO_2, F = 3300 $ml{\cdot}min^{-1}$ were used over a 200 ml bed of $SiMgO_X$ conformed as hollow cylinders and calcined at 500°C in air.

Photocatalytic measurements. The behavior of the photocatalysts comprises both adsorption and photocatalytic properties. Strategies to minimize the adsorption capacity should be designed in order to evaluate the actual photocatalytic performance of the samples. To this end, the extruded plates were crushed and dispersed in 2-propanol. Glass plates were coated with a thin layer of such dispersion and dried at 100ºC. Two set of samples were prepared this way: a sample containing only the absorbent function, with 150 mg of SiMgOx, and TiO_2-$SiMgO_x$ incorporated materials with ratio 1:1 with two different total amounts of material, 150 mg and 40 mg, to evaluate the effective use of the photoactive phase. For comparative purposes, TiO_2 coated samples were prepared as well. Two plates with 20 mg of P25 TiO_2 (Degussa) were prepared, a reference sample, where TiO_2 was deposited directly on the glass plate, and another sample with TiO_2 coated onto the adsorbent.

The glass plates where tested in a continuous plug flow gas phase reactor with a Pyrex glass window of 3 x 10 cm size (length x width). Irradiation (4.4 mW cm^{-2}) was provided by 2 UVA 8 W fluorescence lamps (Philips) which present a maximum emission at 365 nm. H_2S was fed into the reactor from a calibrated H_2S/N_2 gas mixture and diluted with humid air to obtain the desired H_2S and water vapor concentrations. The operating conditions were the following: $[H_2S]$ = 15 ppm, F = 75 ml min^{-1}, T = 30ºC, relative humidity, RH = 30% and P = 1 atm. Outlet concentrations of sulfur compounds were analyzed by a Varian CP-4900 μ-GC.

Selectivity to SO_2 was calculated according to the following equation:

$$S_{SO_2} = \frac{[SO_2]_{outlet}}{[H_2S]_{inlet} - [H_2S]_{outlet}} \cdot 100 \qquad [10]$$

Thermogravimetry and desorption. Thermal gravimetric (TG)-mass spectrometry analysis of the supports was carried out using a Seiko SSC 5200 TG-DTA 320 System coupled to a Thermostar Balzers Instrument. Samples of about 20 mg were treated at room temperature for 20 min under helium (F = 500 ml·min^{-1}). Then, the flow was diminished to 100 ml·min^{-1} and the system was heated to 1000°C, with a heating rate of 5°C·min

[1].

RESULTS AND DISCUSSION

Characterization. Fig. 1 shows the N_2 adsorption – desorption isotherms recorded for the mixed TiO_2-$SiMgO_X$ and pure $SiMgO_X$ extruded plates after temperature treatment at 150°C and 500°C. The isotherms of pure $SiMgO_X$ are of type IV according to the IUPAC classification, which is typical of mesoporous adsorbents showing capillary condensation.[34] Furthermore they exhibit an H2-type hysteresis loop, characteristic of solids having pores of non-uniform size or shape. The $SiMgO_X$ sample calcined at 500°C adsorbs significantly less N_2 at low p/p_0, due to collapse of the porous structure during calcination. At high relative pressures multilayer adsorption takes place and the hysteresis loops indicate the presence of wide mesopores in the range of 30-50 nm.[35] The isotherms of the TiO_2-$SiMgO_X$ composite samples are of the same type, but with a significant decrease in porosities compared to pure $SiMgO_X$ samples, probably induced by the intimate mixing of the TiO_2 powder with the fibrous $SiMgO_X$ clay.

The textural properties of the samples are collated in Table 1. The $SiMgO_X$ plates after drying at 150ºC had a specific surface area of 182 m^2g^{-1}. The surface area was reduced to 130 m^2g^{-1} after treatment at 500ºC. Inspection of the pore volume data revealed that the materials, even before calcination, mainly presented a mesoporous structure and that the contribution from micropores is negligible, as depicted in Table 1. The calcined TiO_2-$SiMgO_X$ plates furthermore present a macroporous structure, seen by MIP analysis, generated during the extrusion process and associated with the interparticulate packing. The surface area of the calcined TiO_2-$SiMgO_X$ composite is 109 $m^2 \cdot g^{-1}$, slightly lower than that of the pure $SiMgO_X$ material.

According to XRD analysis, shown in Fig. 2, the calcined $SiMgO_X$ exhibits crystalline phases of SiO_2 (impurity) and sepiolite anhydride. The TiO_2-$SiMgO_X$ sample contains the same phases and also the typical diffraction pattern of anatase; hardly any rutile phase is observed.

Adsorption capacity. In Fig. 3 the H_2S breakthrough curves of adsorption over the fixed beds of calcined $SiMgO_X$ and TiO_2-$SiMgO_X$ are given. The dynamic adsorption capacities, defined as the amount of H_2S adsorbed at the rupture point - the time where 5 ppm H_2S ($C/C_0 = 0.05$) is observed in the outlet stream of the adsorbent bed- are given in Table 1. As can be seen in Fig. 3, the time before the rupture point is reached is longer for the TiO_2-$SiMgO_X$ sample than for the $SiMgO_X$. These measurements correspond to dynamic adsorption capacities of 0.059 and 0.107 $mmol \cdot g^{-1}$ for the $SiMgO_X$ and the TiO_2-$SiMgO_X$ samples, respectively. Thus, an inherent H_2S adsorption capacity is present in the pure $SiMgO_X$. Furthermore the composite material exhibits an enhanced H_2S capacity, which can result from various phenomena. On one hand, the TiO_2 has adsorptive capacity, which might contribute to the final capacity of the composite. On the other hand, from table 1 it can be appreciated that the macroporosity of the composite material is the double (0.29 cm^3g^{-1}) compared to the pure $SiMgO_X$ (0.14 cm^3g^{-1}). Therefore, since these measurements are carried out under dynamic conditions the rate of surface reaction, due to improved accessibility of the reactants to the surface centers, is enhanced by the introduction of the TiO_2. Most importantly, the results show that the composite material is able to capture H_2S in an efficient manner, and thus can play an important role in a hybrid adsorption/photocatalytic H_2S cleaning system.

In Fig. 4 TGA trace and mass signals from m/z=34 (H_2S) and 64 (SO_2 or S_2) are shown for the $SiMgO_X$ and TiO_2-$SiMgO_X$ 500ºC samples heated in He. The trace signal of m/z=64 can be assigned to S_2 as well as to SO_2, but since the trace of m/z=48 (SO, not shown in figure for clarity) was identical, the observed desorptions originate from SO_2. As it can be seen for both samples, H_2S is mainly released during the heating ramp as physisorbed H_2S at temperatures below 100°C. This suggests that most of the chemisorbed sulfur found at temperature higher than 100ºC is present on the saturated sample in higher oxidation states. A small peak of H_2S might be seen at around 250°C, but since a large SO_2 peak is observed in the same temperature, this H_2S desorption could very well be due to an elemental sulfur decomposition reaction (reverse Claus reaction, eq. 11) involving surface hydroxyl groups, which is known to be occurring on TiO_2 based catalysts.[36]

$$2H_2O(surface) + 3/nS_n(s) \leftrightarrows 2H_2S(g) + SO_2(g) \quad [11]$$

The $SiMgO_X$ sample has three principal SO_2 desorption peaks at 300, 650 and 720°C. The first is probably due to loosely adsorbed SO_2/SO_3^{2-} species, while the desorption peaks at higher temperatures are more likely from sulfate decomposition reactions. It is obvious that in this material sulfur is present in higher oxidation states than -2, which confirms that although most sulfur is released as physisorbed H_2S, there is some oxidation capability as well. The TiO_2-$SiMgO_X$ sample exhibits similar desorption peaks at 250 and 650°C, while the high temperature peak is observed at above 800°C and with a very significant signal. This latter peak is probably related to strongly adsorbed sulfate species on Lewis acid sites.[37] These observations confirm that the TiO_2-$SiMgO_X$ is a better oxidizing catalyst than pure $SiMgO_X$, even in the absence of photons, and prove that beneficial effects are gained by using the hybrid material.

In Fig. 5 the SO_2 breakthrough curve of adsorption over a fixed bed of a pure $SiMgO_X$ sample calcined at 500°C is shown. The $SiMgO_X$ material contains basic centers, which have affinities for the stronger acids present in the gas phase. Since H_2SO_3 ($SO_2 + H_2O$) is a much stronger acid than H_2S, it is expected that the clay material exhibit good SO_2 sorption capacity. As seen in Fig. 5, even in this accelerated test, with 730 ppm SO_2 in the gas phase, the $SiMgO_X$ material exhibits an adsorption capacity of 0.381 $mmol \cdot g^{-1}$, which clearly suggests that under real conditions the sepiolite phase will chemisorb significant amounts of any SO_2 present in the gas phase or produced as a by product on the surface.

Photocatalytic activity. Before the photocatalytic tests, the samples were saturated with H_2S in order to distinguish between adsorption and photocatalytic properties. Firstly a slight decrease of H_2S was observed but due to the small amount of material used, compared to the adsorption tests described above, the H_2S signal rapidly reached the inlet value.

As it was expected, the SiMgOx sample hardly showed any activity under UV irradiation, while TiO_2 containing materials reduced significantly the pollutant presence in the air stream. Pure irradiated TiO_2 oxidizes H_2S very efficiently (Fig. 6, left). Nevertheless, after one hour of irradiation SO_2 appears in the outlet and the selectivity rapidly increases until almost 100% is reached (Fig. 6, right). The same trend was previously observed not only with P25,[17] but also with TiO_2 thin films prepared by sol-gel.[16] SO_2, like all gaseous sulfur compounds, is toxic and malodorous and should be avoided. The use of TiO_2-SiMgOx materials, with both adsorptive and photocatalytic properties, seems to achieve this goal. Both coated and incorporated TiO_2-$SiMgO_X$ composites avoid, or at least retard for 12 hours, SO_2 release into the gas stream, being the first sample almost as efficient as P25. The lower conversion attained with incorporated samples could be attributed to the different TiO_2 distribution and adsorbent amount. The concentration of the TiO_2 on the surface in the coated samples favors the efficient use of incident photons. The fact that incorporated samples prepared with different amounts of photocatalyst showed similar H_2S conversion (figure not shown) indicates that in these samples the reaction rate is limited by the amount of material exposed to photons. On the other hand, for samples with higher adsorbent mass better photocatalytic performance and longer photocatalyst lifetime are expected. The exact role of sepiolite in this system is complex and should be clarified in further research.

CONCLUSION. TiO_2-$SiMgO_X$ composites constitute promising hybrid materials for elimination of H_2S at room temperature. Due to the photocatalytic activity of TiO_2 it is possible to oxidize H_2S into sulfur compounds of higher oxidation states. An important fraction of these oxidized sulfur compounds formed by the photocatalytic process is in the form of volatile SO_2, which might leave the TiO_2 phase as gas and return to the atmosphere as a contaminant. However, by combining the TiO_2 phase with $SiMgO_X$, in the form of incorporated and/or coated materials, the adsorptive capabilities of the clay make it possible to fixate the oxidized sulfur compounds on the solid composite material. Since the sulfur thereafter is deposited as ionic compounds (sulfites/sulfates), these hybrid materials are much easier to regenerate than usual adsorbents, where

elemental sulfur is generally formed, and may recover their activity by washing with water. Since this system works at room temperature, with the use of solar light, the process can be considered as an environmentally benign technology, with great possibilities for use in H_2S removal applications in the future.

ACKNOWLEDGMENT. The authors would like to acknowledge Comunidad de Madrid (DETOX-H2S S-0505/AMB/0406) for financial support.

Table 1:

Sample	treatment (°C/hours)	N_2 Adsorption S_{BET} (m^2g^{-1})	micro (cm^3g^{-1})	meso (cm^3g^{-1})	MIP macro (cm^3g^{-1})	Total pore volume (cm^3g^{-1})
$SiMgO_X$	150/24	182	0.03	0.42	0.10	0.55
$SiMgO_X$	500/4	130	0.00	0.39	0.14	0.53
TiO_2 -$SiMgO_X$	150/24	136	0.01	0.34	0.29	0.64
TiO_2-$SiMgO_X$	500/4	109	0.00	0.31	0.29	0.60

Figures

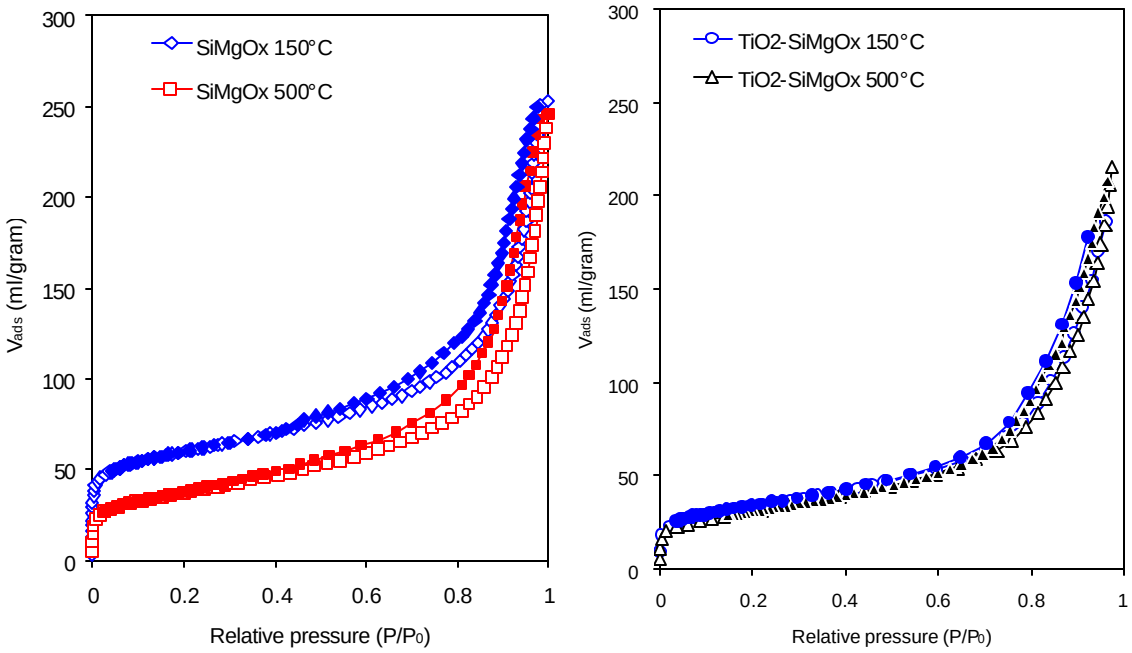

Figure 1: Nitrogen adsorption isotherms of pure $SiMgO_X$ and hybrid TiO_2-$SiMgO_X$ samples treated at 150 and 500°C.

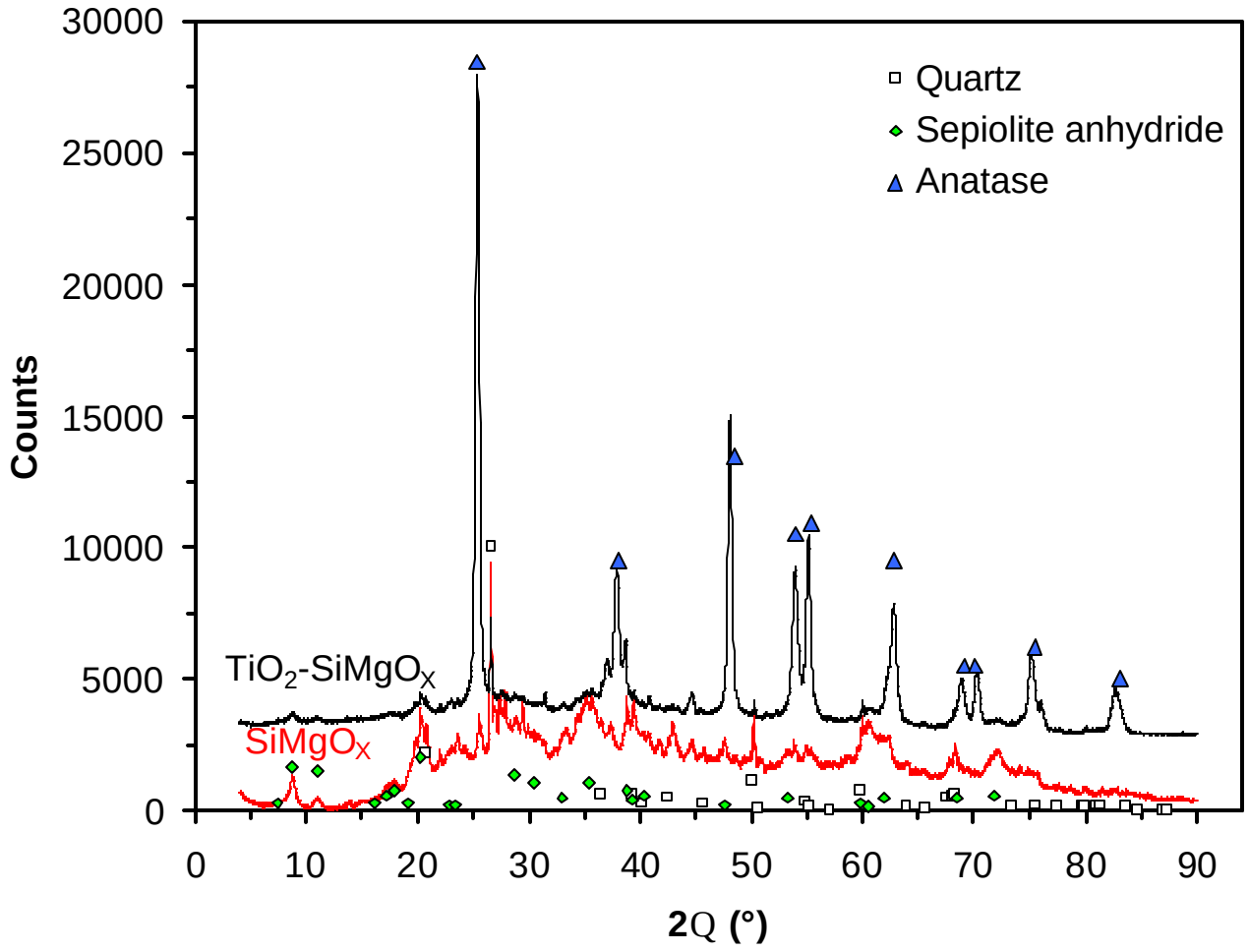

Figure 2: Powder XRD of the $SiMgO_X$ and TiO_2-$SiMgO_X$ supports after calcination at 500°C.

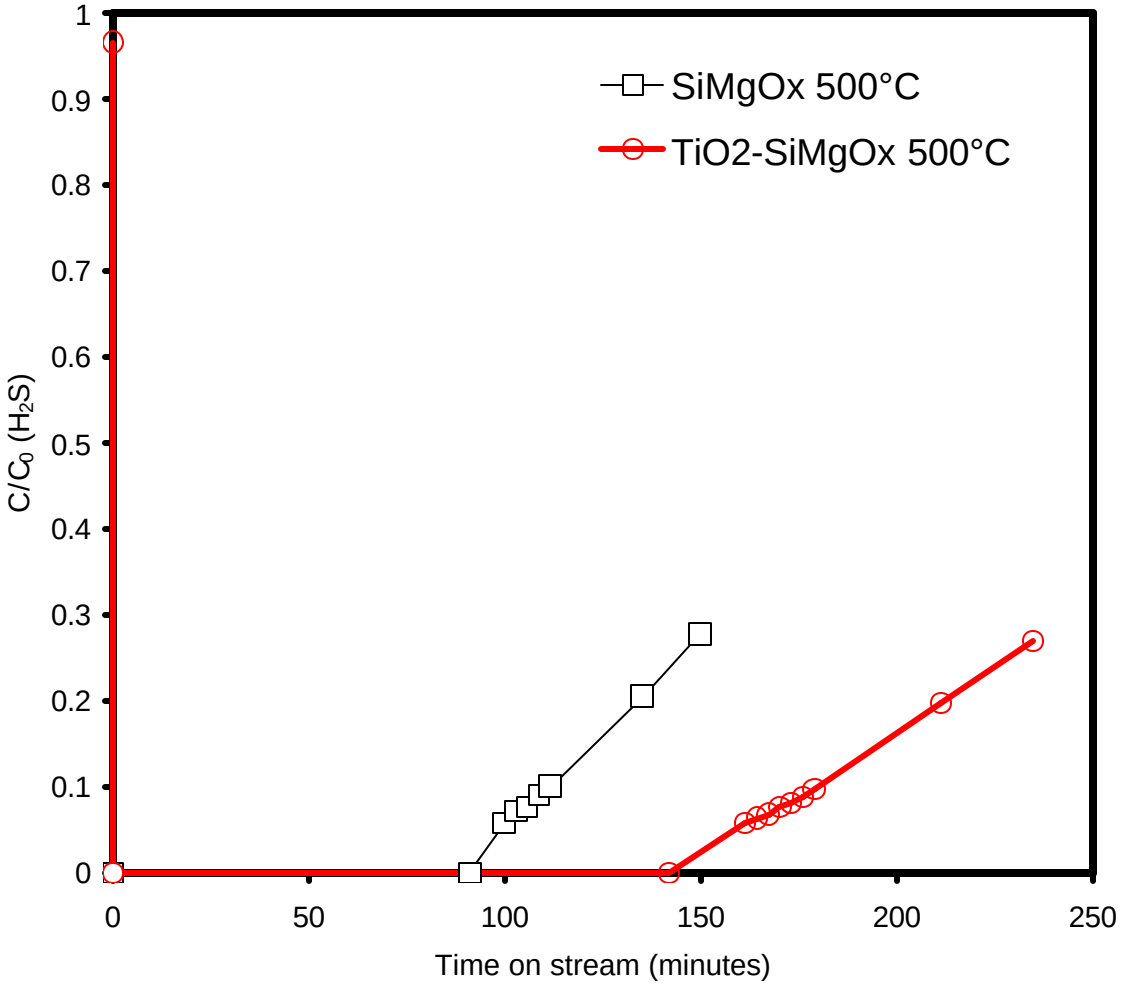

Figure 3: Dynamic adsorption of H_2S with TiO_2-$SiMgO_X$ and $SiMgO_X$ samples after calcination at 500°C.

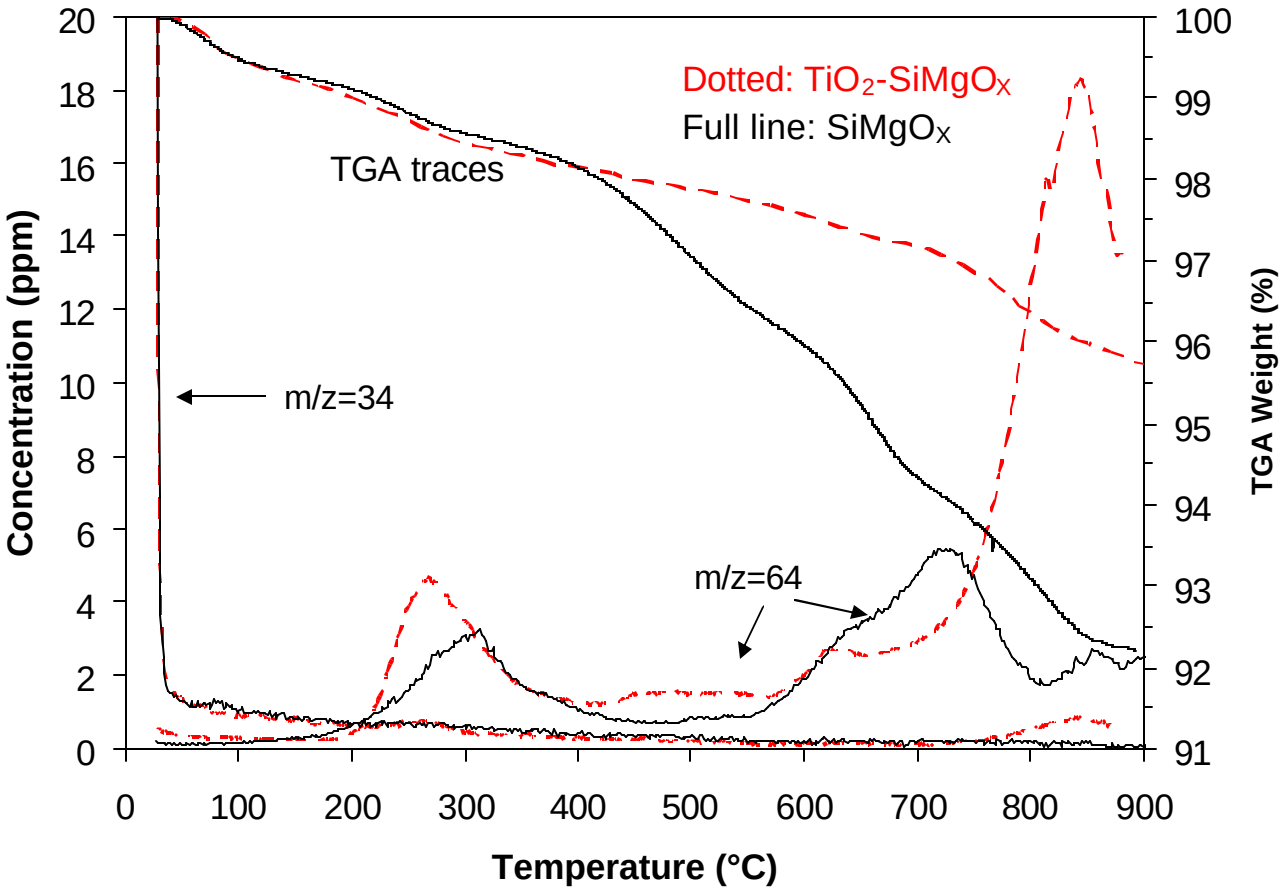

Figure 4: TGA trace and mass spec. signals (curves of m/z = 34 and 64) of the $SiMgO_X$ and TiO_2-$SiMgO_X$ samples (500ºC) after H_2S chemisorption.

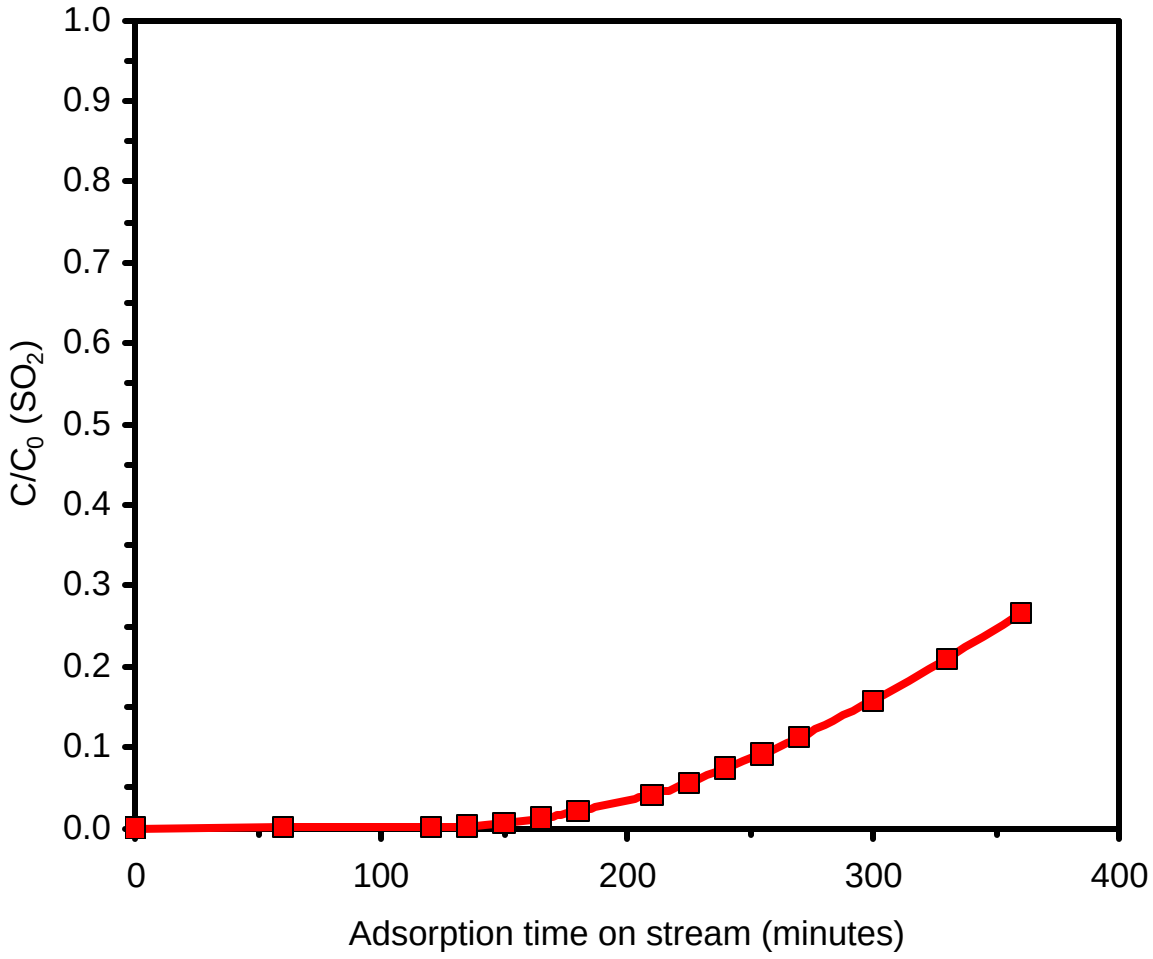

Figure 5: Dynamic adsorption of SO_2 with $SiMgO_X$ (500ºC/4h air).

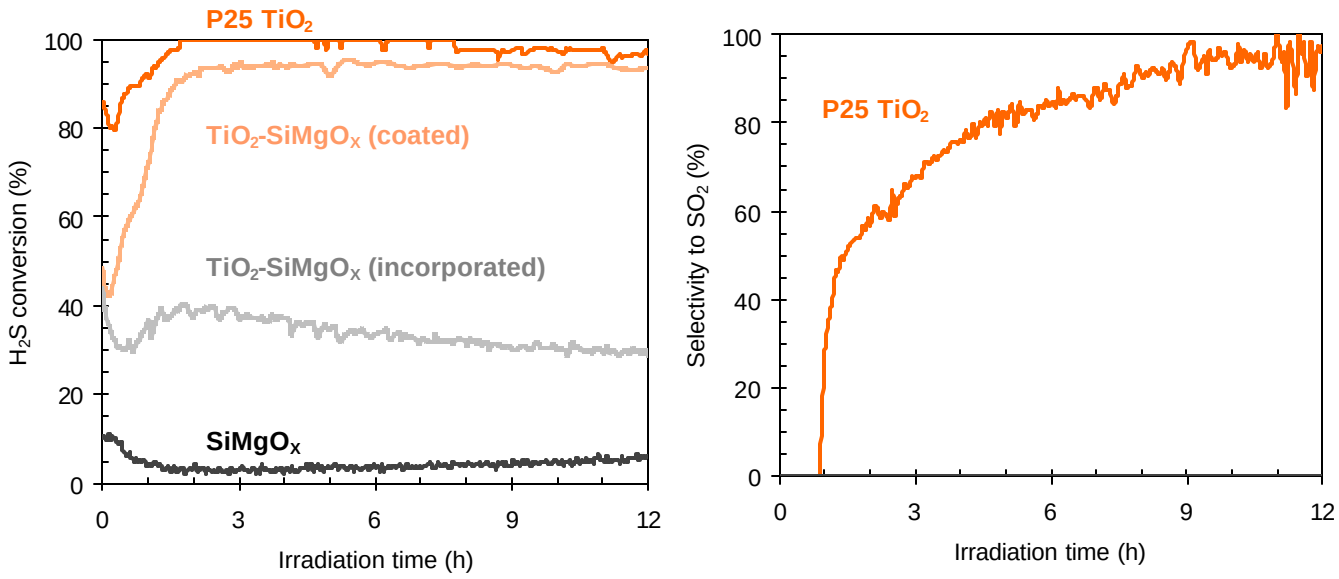

Figure 6: Conversion (left) and selectivity (right) over time during H_2S photocatalytic oxidation with $SiMgO_X$ (solid black), P25 TiO_2 (solid orange), incorporated TiO_2-$SiMgO_X$ (dotted black) and coated TiO_2-$SiMgO_X$ (dotted orange) treated at 500ºC.

REFERENCES

[1] Gostelow, P.; Parsons, S.A.; Stuetz, R.M. Odour measurement in sewage treatment - a review. *Water Research* **2001,** 35, 579.

[2] American Society of Civil Engineers (ASCE), *Odor Control in Wastewater Treatment Plants* WEH, New York, 1995).

[3] Turk, A.; Sakalis, S.; Lessuck, J.; Karamitsos, H.; Rago, O. Ammonia injection enhances capacity of activated carbon for hydrogen sulfide and methyl mercaptan. *Environ. Sci. Technol*. **1989,** 33, 1242.

[4] Bandosz, T. J., Bagreev, A., Adib, F., and Turk, A. Unmodified versus caustics-impregnated carbons for control of hydrogen sulfide emissions from sewage treatment plants. *Environ. Sci. Technol*. **2000**, 34, 1069.

[5] Turk, A.; Sakalis, E.; Rago, O.; Karamitsos, H.; Activated carbon systems for removal of light gases. *Ann. NY Acad. Sci*. **1992**, 661, 221.

[6] Kaliva, A.N.; Smith, J.W. Oxidation of low concentrations of hydrogen sulfide by air on a fixed activated carbon bed. *Can. J. Chem. Eng.***1983**, 61, 208.

[7] Bandosz, T. J. *Fundamentals of Adsorption 6,* Elsevier, Paris, 1998, p. 635.

[8] Steijns, M.; Mars, P. The role of sulfur trapped in micropores in the catalytic partial oxidation of hydrogen sulfide with oxygen. *J. Catal.* 1974, **35** (1974) 11.

[9] Bagreev, A.; Rahman, H.; Bandosz, T.J. Wood-based activated carbons as adsorbents of hydrogen sulfide: A study of adsorption and water regeneration processes. *Ind. Eng. Chem. Res.* **2000**, 39, 3849.

[10] Bagreev, A.; Rahman, H.; Bandosz, T.J. Study of H_2S adsorption and water regeneration of spent coconut-based activated carbon. *Environ. Sci. Technol.* **34** (2000) 4587.

[11] Bandosz, T. On the Adsorption/Oxidation of Hydrogen Sulfide on Activated Carbons at Ambient Temperatures. *J. Coll. Int. Sci*. **2002**, 246, 1.

[12] Fox, M.A.; Dulay, M. Heterogeneous photocatalysis. *Chem. Rev.* **1993**, 93**,** 341.

[13] Carp, O.; Huisman, C.L.; Reller, A. Photoinduced reactivity of titanium dioxide. *Prog. Solid State Chem.* **2004**, 32, 33.

[14] Canela, M. C.; Alberici, R. M.; Jardim, W. F., Gas-phase destruction of H_2S using TiO_2/UV-VIS. *J. Photochem. Photobiol. A* **1998,** 112, 73-80.

[15] Kato, S.; Hirano, Y.; Iwata, M.; Sano, T.; Takeuchi, K.; Matsuzawa, S., Photocatalytic degradation of gaseous sulfur compounds by silver-deposited titanium dioxide. *Appl. Catal. B* **2005,** 57, (2), 109.

[16] Portela, R.; Sanchez, B.; Coronado, J. M.; Candal, R.; Suarez, S. Selection of TiO2-support: UV-transparent alternatives and long-term use limitations for H_2S removal. *Catal. Today* **2007,** 129, 223.

[17] Portela, R.; Canela, M. C.; Sanchez, B.; Marques, F. C.; Stumbo, A. M.; Tessinari, R. F.; Coronado, J. M.; Suarez, S. H2S photodegradation by TiO_2/M-MCM-41 (M=Cr or Ce): deactivation and by-product generation under UV-A and visible light. *Appl.Catal. B* **2008,** 84, 643.

[18] Portela, R.; Suárez, S.; Rasmussen, S.B.; Arconada, N.; Castro, Y.; Durán, A.; Avila, P.; Coronado, J.M.; Sanchez, B.; Photocatalytic-based strategies for H_2S elimination**,** *Catal. Today* (under revision).

[19] Rachel, A.; Subrahmanyam, M.; Boule, P.; Comparison of photocatalytic efficiencies of TiO_2 in suspended and immobilised form for the photocatalytic degradation of nitrobenzenesulfonic acids. *Appl. Catal. B* **2002,** 37, 301.

[20] Sanchez, B.; Cardona, A.I.; Romero, M.; Avila, P.; Bahamonde, A. Influence of temperature on gas-phase photo-assisted mineralization of TCE using tubular and monolithic catalysts. *Catal. Today* **1999**, 54**,** 369.

[21] Alvarez, A. (Singer, A.; Galán, E. Eds.), Elsevier: Amsterdam, Sepiolite: properties and uses, *Developments in Sedimentology*, **1984,** 37, 253.

[22] Bellman, B.; Muhle, H.; Ernst, H. Investigations on health-related properties of two sepiolite samples. *Environ. Health Perspect.* **1997**, 105, 1049.

[23] Suárez, S.; Yates, M.; Petre, A.L.; Martín, J.A.; Avila, P.; Blanco, J. Development of a new Rh/TiO2–sepiolite monolithic catalyst for N2O decomposition. *Appl. Catal. B* **2006**, 64, 302.

[24] Baeza, P.; Villarroel M.; Ávila, P.; López Agudo, A.; Delmon, B.; Gil-Llambías, F.J. Spillover hydrogen mobility during Co-Mo catalyzed HDS in industrial-like conditions. *Appl. Catal. A* **2006**, 304, 109.

[25] Lee, M.C.; Choi, W. Solid Phase Photocatalytic Reaction on the Soot/TiO2 Interface: The Role of Migrating OH Radicals. *J. Phys. Chem. B* **2002**, 106, 11818.

[26] Takeda, N.; Torimoto, T.; Sampath, S.; Kuwabata, S.; Yoneyama, H. Effect of Inert Supports for Titanium-Dioxide Loading on Enhancement of Photodecomposition Rate of Gaseous Propionaldehyde. *J. Phys. Chem.* **1995**, 99, 9986.

[27] Legrini, O.; Oliveros, E.; Braun, A. Photochemical processes for water treatment, *Chem. Rev.* **1993**, 93, 671.

[28] Suarez, S.; Coronado, J.M.; Portela, R.; Martin, J.C.; Yates, M.; Avila, P.; Sanchez, B. On the preparation of TiO_2 - Sepiolite hybrid materials for the photocatalytic degradation of TCE: Influence of TiO2 distribution in the mineralization. *Environ. Sci. Technol.* **2008**, 42, 5892.

[29] Hewer, T. L. R.; Suárez, S.; Coronado, J. M.; Portela, R.; Avila, P.; Sanchez, B., Hybrid photocatalysts for the degradation of trichloroethylene in air. *Catal. Today* **2009,** 13, 302.

[30] Blanco, J.; Avila, P.; Yates, M.; Bahamonde, A. The use of sepiolite in the preparation of titania monoliths for the manufacture of industrial catalysts. In *Preparation of Catalysts VI. Scientific Bases for the Preparation of Heterogeneous Catalysts*, al., G. P. e., Ed. Elsevier Science B.V., 1995, pp 755.

[31] Brunauer, S.; Emmett, P.H.; Teller, E. Adsorption of gases in multimolecular layers, *J. Am. Chem. Soc.* **1938**, 60, 309.

[32] Washburn, E.W. Note on a method of determining the distribution of pore sizes in a porous material. *Proc. Nat. Acad. Sci. USA* **1921**, 7**,** 115.

[33] Rouquerol, J.; Avnir, D.; Fairbridge, C.W.; Everett, D.H.; Haynes, J.H.; Pericone, N.; Ramsay, J.D.F.; Sing, K.S.W.; Unger, K.K. Recommendations for the characterization of porous solids (Technical Report). *Pure Appl. Chem.* **1994**, 66, 1739.

[34] Gregg, S.J.; Sing, K.S.W.. *Adsorption, Surface Area and Porosity.* Academic Press, London, 1991, pp. 110.

[35] Blanco, J.; Petre, A.L.; Yates, M.; Martin, M.P.; Martin, J.A.; Martin-Luengo, M.A. Tailor-made high porosity VOC oxidation catalysts prepared by a single-step procedure. *Appl. Catal. B* **2007**, 73, 128.

[36] Laperdrix, E.; Sahibed-dine, A.; Costentin, G.; Bensitel, M.; Lavalley, J.-C. Evidence of the reverse Claus reaction on metal oxides: Influence of their acid–base properties. *Appl. Catal. B,* **2000**, 27, 137.

[37] Martín, J.C.; Rasmussen, S.B.; Suárez, S.; Yates, M.; Gil-Llambías, F.J.; Villarroel, M.; Ávila, P. Effect of sulphuric acid pretreatment concentration on the behaviour of CoOX/? -Al_2O_3-SO_4 monolithic catalysts in the lean CH_4-SCR process. *Appl.Catal. B* **2009**, 91, 423.